The FEBS Journal

FEBS PRESS science publishing by scientists

A Na^+ A_1A_O ATP synthase with a V-type *c* subunit in a mesophilic bacterium

Dennis Litty and Volker Müller

Molecular Microbiology & Bioenergetics, Institute of Molecular Biosciences, Johann Wolfgang Goethe University, Frankfurt/Main, Germany

Keywords
acetogen; bioenergetics; *Eubacterium*; Na^+ transport

Correspondence
V. Müller, Molecular Microbiology & Bioenergetics, Institute of Molecular Biosciences, Johann Wolfgang Goethe University Frankfurt/Main, Max-von-Laue-Str. 9, Frankfurt 60438, Germany
Tel: +49 69 79829507
E-mail: vmueller@bio.uni-frankfurt.de

(Received 20 September 2019, revised 18 November 2019, accepted 22 December 2019)

doi:10.1111/febs.15193

A_1A_O ATP synthases with a V-type *c* subunit have only been found in hyperthermophilic archaea which makes bioenergetic analyses impossible due to the instability of liposomes at high temperatures. A search for a potential archaeal A_1A_O ATP synthase with a V-type *c* subunit in a mesophilic organism revealed an A_1A_O ATP synthase cluster in the anaerobic, acetogenic bacterium *Eubacterium limosum* KIST612. The enzyme was purified to apparent homogeneity from cells grown on methanol to a specific activity of 1.2 $U \cdot mg^{-1}$ with a yield of 12%. The enzyme contained subunits A, B, C, D, E, F, H, *a*, and *c*. Subunit *c* is predicted to be a typical V-type *c* subunit with only one ion (Na^+)-binding site. Indeed, ATP hydrolysis was strictly Na^+-dependent. *N*,*N*′-dicyclohexylcarbodiimide (DCCD) inhibited ATP hydrolysis, but inhibition was relieved by addition of Na^+. Na^+ was shown directly to abolish binding of the fluorescence DCCD derivative, NCD-4, to subunit *c*, demonstrating a competition of Na^+ and DCCD/NCD-4 for a common binding site. After incorporation of the A_1A_O ATP synthase into liposomes, ATP-dependent primary transport of $^{22}Na^+$ as well as $\Delta\mu Na^+$-driven ATP synthesis could be demonstrated. The Na^+ A_1A_O ATP synthase from *E. limosum* is the first ATP synthase with a V-type *c* subunit from a mesophilic organism. This will enable future bioenergetic analysis of these unique ATP synthases.

Introduction

Despite all the differences in the reactions generating the electrochemical ion potential across the membrane of living cells, the ATP synthase is the universal enzyme present in every living cell to harvest electrochemical energy and transform it into biological useful fuel, ATP [1,2]. All known ATP synthases use the same principle mechanisms of energy conservation and they evolved from a common ancestor [3]. ATP synthases are rotary machines that are composed of two motor domains connected by one central stalk and at least one peripheral stalk. The membrane-embedded motor, A_O, consists of the *c* ring, composed of multiple copies of the *c* subunit, and the stator, subunit *a*. The membrane-embedded domain translocates ions (H^+ or Na^+) across the membrane leading to rotation of the *c* ring against the stator. The resulting rotational energy is transmitted via the central stalk to the A_1 motor which then drives ATP synthesis. This operation is fully reversible, resulting in ATP hydrolysis coupled to ion transport across the membrane [2,4].

Evolutionary, archaeal A_1A_O ATP synthases are more closely related to V_1V_O ATPases, mainly present in vacuoles of eukarya, than to F_1F_O ATP synthases found in bacteria [2]. V_1V_O ATPases are designed by nature as ATP-driven ion pumps and are not able to synthesize ATP *in vivo* [2,5,6]. In most archaeal A_1A_O

Abbreviations
$\Delta\mu Na^+$, electrochemical sodium ion potential; ΔpNa, sodium ion potential; $\Delta\Psi$, membrane potential; DCCD, *N*,*N*′-dicyclohexylcarbodiimide; DDM, *n*-dodecyl-β-maltoside; ETH 2120, *N*,*N*,*N*,*N*′-tetra-cyclo-hexyl-1,2-phenylenedioxydiacetamide; MALDI, matrix-assisted laser desorption/ionization; TCS, 3,3′,4′,5-tetrachlorosalicylanilide.

The FEBS Journal **287** (2020) 3012–3023 © 2019 The Authors. *The FEBS Journal* published by John Wiley & Sons Ltd on behalf of Federation of European Biochemical Societies

ATP synthases, the subunit *c* consists of two transmembrane helices with one ion-binding site as seen in F_1F_O ATP synthases. In the course of evolution, the *c* subunit in eukaryotic V_1V_O ATPases [7,8] underwent gene duplication, giving rise to a proteolipid with four transmembrane helices [9]. Additionally, one ion-binding site was lost resulting in a rotor missing half the number of ion-binding sites. This binding site composition is generally seen as the reason for the inability of V_1V_O ATPases to synthesize ATP *in vivo* [7,10]. Notably, some A_1A_O ATP synthases have a *c* subunit with four transmembrane helices but only one ion-binding site [6]. This structural feature would predict that the enzyme has lost its ATP synthesis capability. However, since no other ATP synthase genes are found in these archaea, one has to postulate that such an enzyme is able to synthesize ATP. This is indeed substantiated by measuring ATP synthesis in whole cells and membrane vesicles [11]. At this point in time, intact A_1A_O ATP synthases could only be purified from hyperthermophilic archaea [12–16]. However, these hyperthermophilic ATP synthases are inactive at temperatures below 80 °C, with temperature optima between 80 °C and 100 °C. Under these conditions, all commonly used liposome systems are inactive and suitable lipids for these conditions could not be obtained so far, despite all efforts.

Inspection of genome sequences from mesophilic bacteria and archaea revealed one gene cluster in *Eubacterium limosum* (T_{opt} = 37 °C) potentially encoding an A_1A_O ATP synthase with an unusual V-type *c* subunit [17]. We have purified the enzyme from membranes of *E. limosum* and will demonstrate that it is a Na^+-dependent A_1A_O ATP synthase containing a V-type like *c* subunit capable of ATP synthesis.

Results

Genome organization, genes, and subunits of the A_1A_O ATP synthase from *E. limosum*

The genes *Eli_2184–2192* encode an enzyme with highest similarity to an archaeal A_1A_O ATP synthase (Fig. 1A). Upstream of the A_1A_O ATP synthase operon on the reverse strand *Eli_2183* (117 bp) encodes for a hypothetical protein with 41% identity to dynein protein 3 of *Saccharomyces cerevisiae* (Table 1). *Eli_2184* is 309 bp long and encodes for subunit H with a molecular mass of 11.4 kDa (Table 1). The encoded protein is 53% similar to subunit H of the A_1A_O ATP synthase from *Methanothermobacter marburgensis*. The next gene of the operon (*Eli_2185*) has a 3 bp overlap with *Eli_2184*. It is 1875 bp long and encodes for subunit *a* of the hydrophobic A_O domain with a molecular mass of 69.8 kDa. The deduced gene product is 31% and 26% identical to the corresponding subunit from *Methanocaldococcus jannaschii* [14] and *Methanosarcina mazei* Gö1 [18], respectively. Most interestingly, 14 bp downstream of *Eli_2185* is the 474-bp-long gene encoding the rotor subunit *c* (*Eli_2186*) with a predicted mass of a 16 kDa and four transmembrane helices (Fig. 1B). The similarity/identity to subunit *c* of *Pyrococcus furiosus* is 51/35%. Recently, we have shown that the *c* subunit from *P. furiosus* has indeed four transmembrane helices but only one ion (Na^+)-binding site (Q...ET) [19] which is also conserved in *Thermococcus onnurineus* and in subunit *c* of *E. limosum*. As in *P. furiosus*, there is no second proton or sodium ion-binding site conserved. *Eli_2187* (606 bp) is located 36 bp downstream of *Eli_2186*, and the deduced protein (22.6 kDa) is annotated as subunit E of V_1V_O ATPases. No significant homology to the corresponding protein sequence of subunit E in A_1A_O ATP synthases was found. Four base pair downstream of *Eli_2187* is the 972-bp-long gene *Eli_2188* which encodes for a subunit C with a molecular mass of 36.4 kDa. The identity/similarity of the deduced protein is 26/47% to subunit C of the A_1A_O ATP synthase from *P. furiosus* [12]. Ten base pair downstream of *Eli_2188* is 318-bp-long *Eli_2189* which encodes a polypeptide with a molecular mass of 11.3 kDa. 51/27% of the residues are similar/identical to subunit F of the A_1A_O ATPase from *M. barkeri* [20]. *Eli_2190* (1806 bp) is located 26 bp downstream of *Eli_2189* and encodes for subunit A with a molecular mass of 66.8 kDa. The deduced gene product is 59% identical to the corresponding subunit from *M. jannaschii* and *T. onnurineus*. *Eli_2191* (1410 bp) encodes for subunit B with a molecular mass of 52.3 kDa. 71, 67, and 30% of the residues are identical to subunit B of the A_1A_O ATPase from *P. furiosus*, *T. onnurineus*, and *M. barkeri*, respectively. Four base pair downstream of *Eli_2191* is *Eli_2192* with a length of 636 bp. The protein has a molecular mass of 29.4 kDa. Sequence alignments showed 42% and 39% identity to subunit D of *M. jannaschii* and *T. onnurineus*, respectively. The next gene downstream of the putative ATP synthase operon *Eli_2193* (138 bp) is located in 3′ → 5′ direction. For this gene, no homologues were found.

Purification of the A_1A_O ATP synthase from *E. limosum*

To determine the effect of the growth substrate on ATPase activity, *E. limosum* KIST612 was grown on complex medium with 50 mM glucose, 50 mM

A

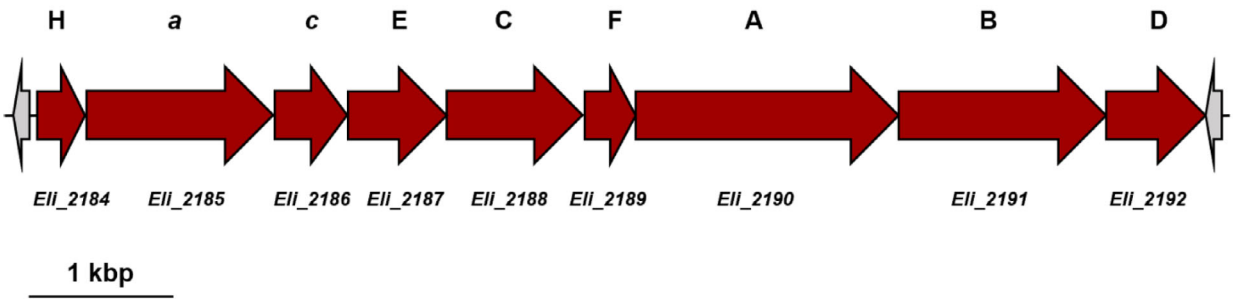

B

```
E.limosum                MSLGLALAIFGAAIAAGLAGIGSAKGVQISGEAAAGVVAERPEMFGKMLVLQALPGTQGI   60
P.furiosus               -MDPIVYVALGMALGAGIAGAASSFGVGIAGAAAAGAVAEDERNFRNALILEGLPMTQSI   59
T. onnurineus            -MDPIVYVSLGAALAAGIAGAASAFGVGIAGAAAAGVVAEDEKNFKNALILEGLPMTQSI   59
                             :. . :* *:.**:** .*: ** *:* ****.***  . * : *:*:.** **.*

E.limosum                YGFLTAVLIMVQIGILGGTPLDLSLYQ-------GMSFLAAGFPIGIVGLLSGIAQGKAA   113
P.furiosus               YGLITLFLIGMTAGVIGGGGFKFAEPT-TENLIKSAILFGAGLLVGLTGL-SAIPQGIIA   117
T. onnurineus            YGLITLFLILMVSGILGG-GFKFTDPNNMDNIVKSAILLGAGLTVGLTGL-SAIPQGIIA   117
                         **::* .** :  *::**  :.::          .  ::.**: :*:.** *.* **  *

E.limosum                AASIHMTAKDESAFAKGITITAIVETYAILALLVSILLIYSIQL-    157
P.furiosus               SSGIGAVSKNPKTFTQNLIFAAMAETMAIFGLVGAILLIMSL---    159
T. onnurineus            SASIGAVAKNPKTFTQGIIFSAMAETMAIFGLVGALIMIVTGVGF    162
                         ::.*  .:*: .:*::.: ::*:.** **:.*: ::::* :
```

Fig. 1. Genetic organization of the A_1A_O ATP synthase operon from *Eubacterium limosum* and alignment of subunit *c*. The A_1A_O ATP synthase operon of *E. limosum* comprises nine genes. The genes of the ATP synthase operon are highlighted in red (A). The *c* subunit of the putative A_1A_O ATP synthase has a conserved Na^+-binding motif. The amino acid sequence of the *c* subunit of the putative A_1A_O ATP synthase from *E. limosum* (accession number: E3GNI4) was aligned with the sequences of subunit *c* of *Pyrococcus furiosus* (accession number: Q8U4B0) and *Thermococcus onnurineus* (accession number: B6YV10). The Na^+-binding motif (Q. . .ET) is highlighted in yellow. The sequence alignment was performed by using CLUSTAL OMEGA (Dublin, Ireland) (B).

Table 1. Properties of the A_1A_O ATP synthase subunits

Gene	Subunit	Residues	M_r	pI
Eli_2184	H	102	11 406	4.81
Eli_2185	*a*	624	69 757	4.8
Eli_2186	*c*	157	15 720	5.64
Eli_2187	E	201	22 574	4.83
Eli_2188	C	323	36 377	5.19
Eli_2189	F	105	11 283	4.89
Eli_2190	A	601	66 841	4.78
Eli_2191	B	469	52 296	4.85
Eli_2192	D	211	23 986	7.73

methanol, 50 mM formate, 101 kPa $H_2 + CO_2$, or 101 kPa CO as sole carbon and energy source. Cells were harvested during exponential growth, washed membranes were prepared, and ATP hydrolysis was determined. Washed membranes of $H_2 + CO_2$-grown cells had the highest ATPase activity of 68.3 $mU \cdot mg^{-1}$. The activity of washed membranes from methanol-, formate-, and CO-grown cells was similar and slightly below the latter one (54, 41.3, and 50.7 $mU \cdot mg^{-1}$). Membranes from glucose-grown cells showed the lowest activity with 24 $mU \cdot mg^{-1}$. Due to the low yield of cell mass from $H_2 + CO_2$-grown cultures (final $OD_{600} = 0.4$), methanol was selected as growth substrate (final $OD_{600} = 1.2$) for large-scale cultivation. For purification of the A_1A_O ATP synthase, washed membranes of around 15 g cells (wet mass) were prepared and solubilized with 1 mg *n*-dodecyl-β-maltoside (DDM) per mg membrane protein. The ATP synthase was further purified by a sucrose density gradient (20–65%), and the subsequent purification by an anion exchange chromatography step (DEAE) as well as a size-exclusion chromatography (Superose 6 column) resulted in 23.6-fold enrichment

of the activity with a specific activity of 1277 mU·mg^{-1} and a yield of 12.2% (Table 2).

Subunit composition of the A_1A_O ATP synthase from *E. limosum*

The preparation contained 13 proteins (Fig. 2) with apparent molecular masses of 67 kDa (subunit A), 58 kDa (subunit B), 39 kDa (subunit C), 26 kDa (subunit D), 25 kDa (subunit E), 11 kDa (subunit F), 12 kDa (subunit H), and 14 kDa (subunit *c*). As seen before with A_1A_O ATP synthases from hyperthermophilic archaea, there is a protein above subunit A which could be a SDS-resistant *ac* subcomplex [12,15]. Single subunit *a* was not detected. The identity of the subunits was proven by MALDI-TOF-MS (Fig. 3) and immunological with antibodies generated and specific against the purified subunits. The 14 kDa protein was identified as subunit *c* by peptide mass fingerprinting. Notably, the loops connecting TMH1 and 2 as well as TMH3 and 4 were detected, demonstrating that subunit *c* indeed contains four transmembrane helices (Fig. 4).

Basic biochemical properties of ATP hydrolysis

ATPase activity was detected over a pH range between 5.0 and 9.0, with optimal activity between pH 7.0 and 7.5 (Fig. 5A). pH values lower than 6.0 and higher than 8.0 decreased the activity very strongly (9.5% activity at pH 5.0, 10% activity at pH 9.0). ATP hydrolysis activity was optimal between 30 °C and 40 °C (Fig. 5B). After 45 °C, the activity decreased sharply. Methanol stimulated ATP hydrolysis activity as described before [21] (Fig. 5C). Optimal activity was determined with 20% methanol.

Na^+ dependence of ATP hydrolysis

ATP hydrolysis was strictly dependent on the Na^+ concentration of the assay buffer (Fig. 6). At the contaminating amount of 71 μM Na^+, ATP hydrolysis was only 326 mU·mg^{-1} but activity was stimulated fourfold by the addition of Na^+. The Na^+ dependence followed a classical Michaelis–Menten kinetics; full activity was observed at 0.6 mM and half maximal was at 0.3 mM. The addition of Li^+ also stimulated ATP hydrolysis; full activity was observed at 2 mM and half maximal activity was at 1 mM. K^+ did not stimulate ATP hydrolysis.

DCCD and Na^+ compete for binding to subunit *c*

DCCD is a common inhibitor for ATP synthases that covalently binds to the highly conserved protonated carboxylate (E138 in helix 4) in subunit *c*, thereby inhibiting proton or Na^+ binding and transport [22,23]. In all known Na^+ ATP synthases, the access of DCCD is blocked in the presence of Na^+, thus reducing the inhibitory effect of DCCD on the enzyme [12,19,24–26]. DCCD inhibited the A_1A_O ATP synthase from *E. limosum* with half maximal inhibition at 80 μM DCCD (Fig 7). When the enzyme was preincubated with Na^+, DCCD inhibition was relieved. NCD-4 is a fluorescent analogue of DCCD and bound to subunit *c* (Fig. 8). Preincubation with Na^+ prevented NCD-4 binding. These data are consistent with the proposal that Na^+ is the coupling ion of the A_1A_O ATP synthase from *E. limosum*.

Na^+ transport and ATP synthesis in proteoliposomes

In order to unequivocally proof Na^+ transport by the A_1A_O ATP synthase, the enzyme was reconstituted into liposomes consisting of phosphatidylcholine type II S from soybeans. Liposomes were generated by sonification [27]. Upon addition of ATP, $^{22}Na^+$ was transported into the lumen of the vesicles with a rate of 0.6 nmol Na^+·min^{-1}·mg^{-1} protein, leading to a final accumulation of 9.2 nmol Na^+·mg^{-1} protein (Fig. 9). $^{22}Na^+$ transport was not observed in the absence of ATP or in the presence of the sodium ionophore *N*,*N*,*N*,*N*′-tetra-cyclo-hexyl-1,2-phenylenedioxydiacetamide (ETH 2120). The protonophore 3,3′,4′,5-tetrachlorosalicylanilide (TCS) slightly stimulated $^{22}Na^+$ transport.

Table 2. Purification of the Na^+ A_1A_O-ATP synthase from *Eubacterium limosum* KIST612

Step	Total protein (mg)	Volume (mL)	Total activity (U)	Specific activity (mU·mg^{-1})	Purification (*x*-fold)	Yield (%)
Washed membranes	272	14	14.69	54	1	100
Solubilizate	124	8	11.9	96.2	1.8	81
Sucrose gradient	23	28	7.08	308	5.7	48.2
DEAE	4.1	20	2.89	703	13	19.7
Gel filtration	1.4	1	1.79	1277	23.6	12.2

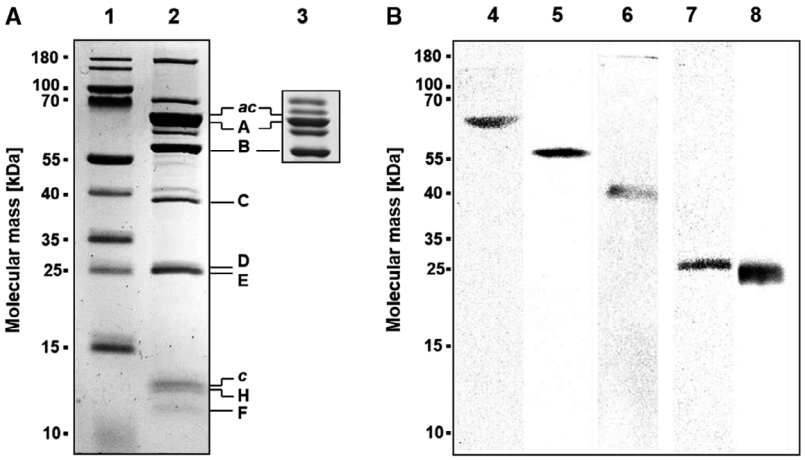

Fig. 2. Subunit composition of the Na^+-A_1A_O-ATP synthase from *Eubacterium limosum* KIST612. Twenty microgram of protein was separated by SDS/PAGE and stained with Coomassie (A) or blotted against specific antibodies (B). 1: Prestained PageRuler™; 2: purified enzyme (12.5% SDS/PAGE); 3: further separation of subunits *ac* and A (15% SDS/PAGE); 4–8: detection of subunits A (4), B (5), C (6), D (7), and E (8) via specific antibodies generated against each subunit (1 : 10 000). The remaining subunits were verified by MALDI-MS. The data are the result of three independent experiments (n = 3).

These data are consistent with a primary and electrogenic Na^+ transport catalyzed by the A_1A_O ATP synthase.

Next, we investigated whether the enzyme is capable of ATP synthesis despite its V-type like *c* subunit. Therefore, the enzyme was again reconstituted into liposomes and an electrochemical Na^+ potential ($\Delta\mu Na^+$) of around 270 mV was applied. $\Delta\mu Na^+$ was generated by a sodium ion potential (ΔpNa) of 75 mV combined with a K^+/valinomycin diffusion potential of around 195 mV. Upon addition of 2 μM valinomycin, ATP was synthesized with a rate of about 54 $nmol \cdot min^{-1} \cdot mg^{-1}$ protein (Fig. 10). The data demonstrate that the A_1A_O ATP synthase with its V-type like *c* subunit from *E. limosum* is capable of ATP synthesis.

Discussion

Many archaea like methanogens, *Thermococcus*, or *Pyrococcus* live under extreme conditions: at high temperatures of > 80 °C, sometimes paired with another extreme, a metabolism that allows for the production of only a small fraction of an ATP per mol of substrate oxidized [28–30]. This life at the thermodynamic limit requires adaptions in the ATP-generating mechanisms. ATP is synthesized exclusively or in addition by a chemiosmotic mechanism that involves unusual respiratory enzyme such as membrane-bound, ion-translocating hydrogenases (progenitors of complex I) or a formate dehydrogenase [30,31]. Often, the free energy change is so small that it allows for the translocation of only one ion per mol of substrate oxidized, sometimes, as in the case of *T. onnurineus*, even less than that [31]. Special adaptions in the ATP synthase also contribute to this lifestyle. One adaption is the use of Na^+ instead of H^+ as coupling ion, the other a *c* ring with a reduced number of ion translocation sites [28,29,32]. This would allow the enzyme to synthesize ATP at lower costs; however, this would only work if the phosphorylation potential in these cells is also lower [33].

In F_1F_O ATP synthases, the minimal ion/ATP ratio is 2.7, restricted by the minimal number of 8 *c* subunits with two transmembrane helices to form a ring structure. However, a doubling of the size of the individual *c* subunits forming the ring increases the stability of the ring structure due to its longer size and possibly allows a further reduction of the ion/ATP ratio. Indeed, the *c* ring of the A_1A_O ATP synthase of *P. furiosus* is proposed to have 10 [13] or 9 [34] subunits.

Measurements of energetic parameter such as phosphorylation potential, membrane potential, and ion transport are scarce in these hyperthermophilic archaea, due to their difficult cultivation and inherent problems of measuring these values at temperatures at 80–100 °C. A solution to this dilemma comes with acetogenic bacteria such as *Acetobacterium woodii* or, here, *E. limosum*. Both are mesophiles but like most other acetogenic bacteria live at the thermodynamic edge of life. *A. woodii* grows heterotrophically but also autotrophically on $H_2 + CO_2$ [35]. The phosphorylation potential in these cells was measured to be much below the 'textbook-knowledge' value of 60 $kJ \cdot mol^{-1}$: 37.9 ± 1.3 $kJ \cdot mol^{-1}$ for fructose, 32.1 ± 0.3 for $H_2 + CO_2$, and 30.2 ± 0.9 for CO [36]. This would allow ATP synthesis with only a fraction of ions. Indeed, the *c* ring of the Na^+ F_1F_O ATP synthase from *A. woodii* is unique since it contains one V-type *c* subunit along with nine F-type *c* subunits, the first and so far, only F/V-hybrid motor found in nature [37]. The

Subunit H

MSILDSINKA EERAAEMRSE AKAKARETLR QAEAEAREKG DALILEAKEA
SEAVLLQEEA LAEKEMERVL HDAGLADEKM AENARTRVPK AVEFILERVE
TQ

Subunit *a*

MIIPMKKAKL IALKEDKEAL LLSLQRCGEF MAIPPDEETE QTAKNEQIDL
DVQQADAMLR FMQRYQKKKS FFSDRPVYGY DEFIKRNEKG EALVQETSAI
SDKLSAAHSE IMTLKSECSQ LEPWLSMDVP IEELRPTQYT NFHIGYLPPL
VHEEIVAAVA EHNAEIQLFG KTAEGQAALI VSFMEDDAAL SDNIKVLGFV
EASLPRVTGT ASEISKSNQE KIELLEKDIE SYEKQMAELA GSQQELELLS
EQYKAEQERQ SVKFMETVET VCVEGWVRND RMESVENAVS QVTDVYDLEY
SDPEEGEQPP TALKNKKFWK PFESITDMYS PPKPGTIDPT PVSAPWFWVI
FGMMMGDFGY GALMAIIFGL MKKIMKPKGQ FGMLVTLLFY SSITTMIFGI
LFGSYFGETF HPILFSPLDN PVAMLIFSLV IGVLHIFSGM AIKIVEQVRA
GHVLDAIFDQ VSWMLLIAGA GLIFLEQTRT VGMVLAIVGA VIILFTAGRE
KKNIVGKAFG GIMGLYDVTS YLSDILSYAR ILALGLATGV IAMVMNILAG
MVQINVLGFI LSLVIYFIGH AFNITMSLLS AYVHDSRLQY IEFFNKFYDG
GGYNFEPLAI QTKSIDVIDN SKEV

Subunit F

MSEQAKLAVI GDQDSIMVFQ ALGVRTVYAN AAKDIEKAIH ALAKEETAVI
YITEQAAALV PEAIEKYKTE PFPAIIPIPN RFGTNGLGMK GIQDNIEKAI
GADIL

Fig. 3. Analysis of the amino acid sequence of subunit H, *a*, and F of *Eubacterium limosum*. To analyze the amino acid sequence of each subunit, the proteins were excised from a 12.5% Coomassie-stained SDS gel and analyzed by MALDI-TOF-MS. The identified amino acids are highlighted in yellow.

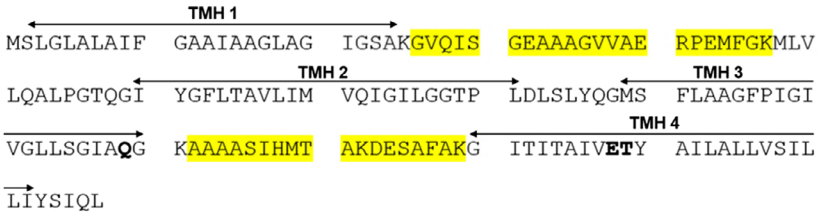

Fig. 4. Analysis of the amino acid sequence of subunit *c* of *Eubacterium limosum*. To analyze the amino acid sequence of subunit *c*, the protein was excised from a 12.5% Coomassie-stained SDS gel and analyzed by MALDI-TOF-MS. Subunit *c* contains four transmembrane helices (TMH1–4) and one Na^+-binding site. The identified amino acids are highlighted in yellow. The sodium ion-binding motif is indicated in bold.

ATP synthase of *E. limosum* has a V-type like *c* subunit, but, as shown here, is able to synthesize ATP. With this mesophilic enzyme in hand, the road is paved to analyze the dependence of ATP synthesis on energetic parameters in these unusual organisms whose metabolism is considered to be maybe the first metabolic scenario on early Earth.

Materials and methods

Cultivation of cells and preparation of washed membranes

Eubacterium limosum KIST612 was cultivated in anoxic phosphate-buffered basal medium (PBBM) or carbonate-buffered

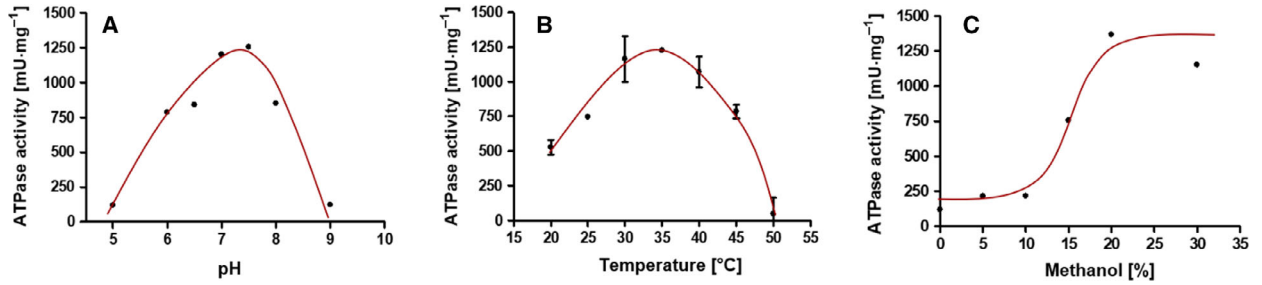

Fig. 5. Basic biochemical properties of the A_1A_O-ATP synthase from *Eubacterium limosum*. The buffer used for the pH optima determination contained 50 mM MES, 50 mM Tris, 50 mM HEPES, 50 mM CHES, 10 mM $MgCl_2$, 20% methanol with a pH as indicated and 10 μg enzyme. The reaction temperature was set to 37 °C (A). The temperature optimum was determined with a buffer containing 100 mM Tris, 100 mM maleic acid, 10 mM $MgCl_2$, 20% methanol (v/v), pH 7.3, and 10 μg enzyme. After incubating the enzyme for 3 min at the temperature as indicated, the reaction was started by addition of a final concentration of 2.5 mM Na_2-ATP (B). The dependence on methanol was measured with 10 μg enzyme in the same buffer at 37 °C. The enzyme was incubated for 3 min at 37 °C, and the reaction was started by addition of ATP to a final concentration of 2.5 mM (C). The data represent the mean and standard deviation of three independent experiments (n = 3), each performed in triplicate.

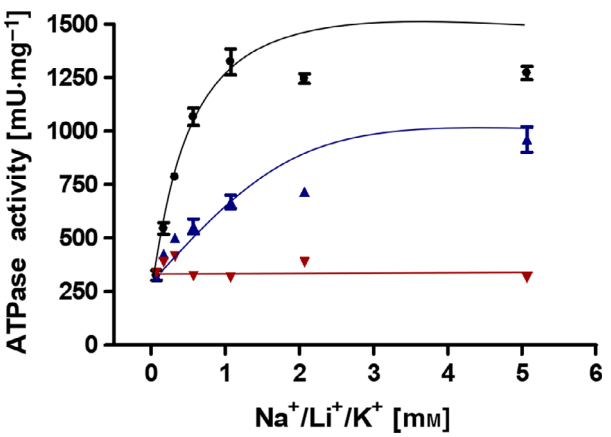

Fig. 6. Na^+ dependence of ATP hydrolysis by the A_1A_O-ATP synthase from *Eubacterium limosum*. ATPase activity was measured at 37 °C. The buffer contained 100 mM Tris, 100 mM maleic acid, 10 mM $MgCl_2$, 20% methanol, pH 7.3, and 20 μg enzyme. The concentration of Na^+ in the sodium-free buffer was determined to be 71 μM by using a Na^+-selective electrode. NaCl (black, circles), LiCl (blue, triangles up), or KCl (red, triangles down) was added as indicated. The reaction was started by addition of 2.5 mM Tris-ATP (final concentration). The data represent the mean and standard deviation of three independent experiments (n = 3), each performed in triplicate.

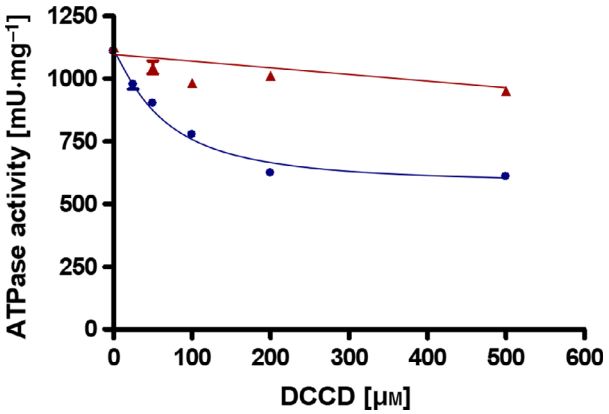

Fig. 7. Inhibition of ATP hydrolysis by DCCD and its relieve by Na^+. The buffer contained 100 mM Tris, 100 mM maleic acid, 10 mM $MgCl_2$, 20% methanol, pH 6.3, and 20 μg enzyme. After preincubation of the enzyme with increasing concentrations of DCCD (0–500 μM, solved in ethanol) in the presence (red, triangles up) or absence of Na^+ (blue, circles) for 25 min at room temperature and incubation for 3 min at 37 °C, the reaction was started by addition of 2.5 mM Tris-ATP (final concentration). The data represent the mean and standard deviation of three independent experiments (n = 3), each performed in triplicate.

basal medium (CBBM) at 37 °C as described previously [38]. Glucose (50 mM), methanol (50 mM), formate (50 mM), H_2 + CO_2 [101 kPa, 80 : 20 (v/v)], or CO (101 kPa) was used as growth substrates. The cells were harvested in midexponential growth phase by centrifugation (Beckman Avanti J25, JA10 rotor, Beckmann Coulter, Krefeld, Germany). For the preparation of washed membranes, around 1 g (wet mass) of cells grown on different substrates was suspended in 5 mL of buffer A (50 mM Tris/HCl, 10 mM $MgCI_2$, 420 mM sucrose, pH 7.5). Lysozyme (20 mg·g^{-1} cells) was added, and the suspension was incubated for 1 h at 37 °C. All subsequent steps were performed at 4 °C unless indicated otherwise. After addition of PMSF (final concentration: 0.5 mM) and a few crystals of DNase I, the resulting protoplasts were disrupted by passing three times through a French pressure cell press at 110 MPa (SLM Aminco, SLM Instruments, Urbana, IL, USA). After dilution with four volumes of buffer A, cell debris was removed by centrifugation (Beckman Avanti J25, JA14 rotor, 10 000 ***g***, 20 min). The membranes were separated from the cytoplasm by centrifugation of the collected cell-free crude extract (Beckman Optima L90-K, 70.2 Ti rotor, 149 000 ***g***, 45 min, Beckmann

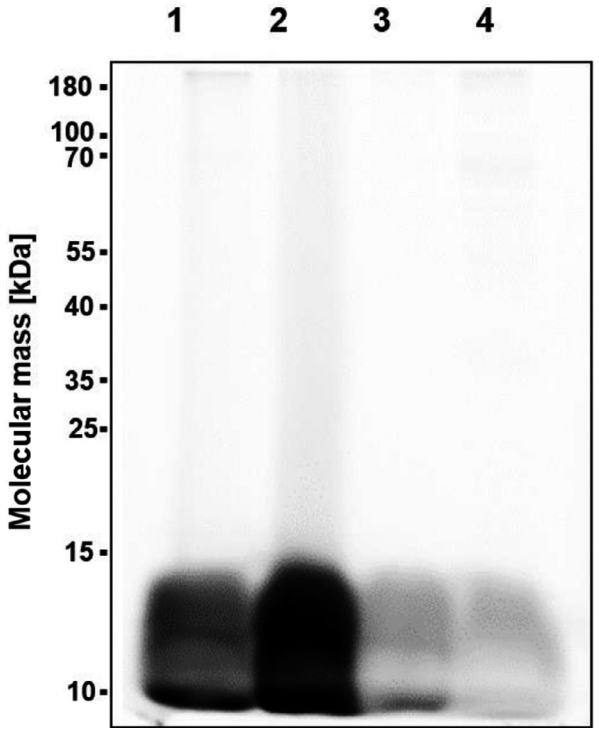

Fig. 8. Na^+ protects labeling of subunit *c* by NCD-4. The purified A_1A_O-ATP synthase (10 μg) was incubated overnight at room temperature with different concentrations of NCD-4 and in the presence or absence of 200 mM NaCl. The samples were separated by SDS/PAGE (12.5%), and the labeled *c* subunit was detected by UV radiation. 1: Incubation with 60 nmol NCD-4; 2: incubation with 200 nmol NCD-4; 3: incubation with 60 nmol NCD-4 and 200 mM NaCl; 4: incubation with 200 nmol NCD-4 and 200 mM NaCl. The data represent the result of three independent experiments (n = 3).

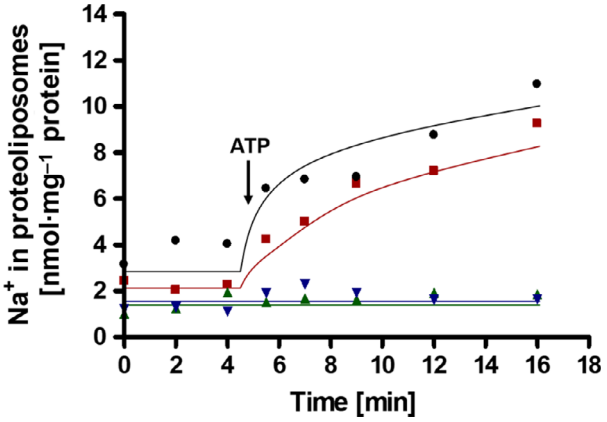

Fig. 9. Na^+ translocation by the purified A_1A_O ATP synthase. Proteoliposomes containing 600 μg of the reconstituted A_1A_O-ATP synthase (30 : 1) in 100 mM Tris buffer (pH 7.3) with 10 mM $MgCl_2$ were preincubated 30 min with ^{22}Na and the presence of either 30 μM of the sodium ionophore ETH 2120 (blue, triangles down) or 30 μM of the protonophore TCS (black, circles). After 30-min preincubation at room temperature, the assay was incubated for additional 5 min at 37 °C. The reaction was then started by adding Tris-ATP to a final concentration of 2.5 mM. (red, squares) contained proteoliposomes without ionophors. In the green plot (triangles up), neither ionophors nor ATP were added. The result represents two independent experiments (n = 2), each performed in duplicate.

Coulter Krefeld, Germany) and washed twice with buffer B (50 mM Tris/HCI, 10 mM $MgCI_2$, 20 mM NaCl, pH 7.5).

Purification of the A_1A_O ATP synthase from *E. limosum*

For purification of the ATP synthase, cells of *E. limosum* KIST612 were grown in CBBM with 50 mM methanol as substrate at 37 °C under anoxic conditions in two 20-L carboys (Glasgerätebau Ochs, Bovenden-Lenglern, Germany). All purification steps were performed at 4 °C under oxic conditions. Methanol-grown cells were harvested in midexponential growth phase by continuous centrifugation (Heraeus centrifuge, Stratos, Hanau, Germany; HCF 22.300 rotor), and washed membranes of around 15 g cells (wet mass) suspended in 30 mL buffer A were prepared as described above. The washed membranes were resuspended in 8 mL buffer B. To solubilize the ATP synthase, 1 mg *n*-dodecyl-β-D-maltoside (DDM) (Carl Roth, Karlsruhe, Germany) per milligram of membrane protein was added and incubated under shaking for 2.5 h. The remaining membranes were removed by ultracentrifugation (180 000 ***g***, 30 min), and the solubilizate was loaded onto a sucrose gradient (20–65%) and centrifuged for 19 h in a vertical rotor (Beckman Optima L90-K, VTi50 rotor, 152 624 ***g***). Each sucrose gradient fraction was tested for ATPase activity. The fractions of sucrose gradient with the highest ATPase activity were pooled and applied to anion exchange chromatography column. Therefore, DEAE Sepharose Fast Flow (GE Healthcare, Uppsala, Sweden) was equilibrated with buffer C [100 mM HEPES, 5 mM $MgCl_2$, 10% (v/v) glycerol, pH 7.3] and a salt gradient (0.15–0.4 M NaCl) in buffer C at a flow rate of 1 mL·min^{-1} was used for elution. The ATP synthase eluted at around 0.25 M NaCl. Fractions containing the ATP synthase were pooled and concentrated to a volume of 1 mL (Vivaspin 20 columns, 100 kDa MWCO; Sartorius, Goettingen, Germany). To further purify the sample, an additional size-exclusion chromatography was performed. In aliquots of 0.5 mL, the protein was applied onto a Superose 6 column (10/300 GL; GE Healthcare, Uppsala, Sweden) that was equilibrated with buffer D [100 mM HEPES, 250 mM NaCl, 5 mM $MgCl_2$, 10% (v/v) glycerol, 0.02% (w/v) DDM, pH 7.3]. The purified ATP synthase eluted with buffer D with a flow rate of 0.5 mL·min^{-1}. For experiments under Na^+-free conditions, the protein was eluted with buffer D without addition of NaCl. The concentration of Na^+ was determined by using a Na^+-selective electrode (ORION™ 8411BN ROSS®; Thermo Fisher Scientific

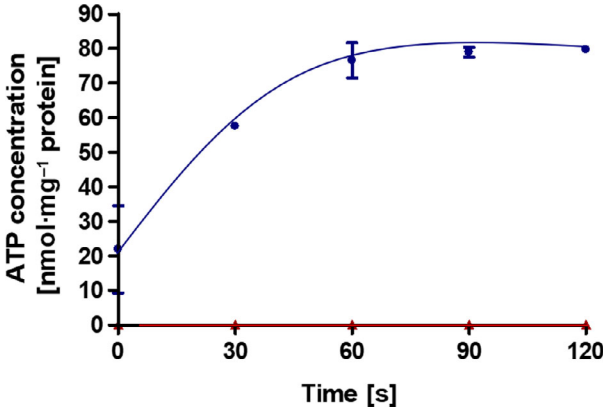

Fig. 10. $\Delta\mu Na^+$-driven ATP synthesis by the purified A_1A_O ATP synthase. Proteoliposomes containing 250 μg of the reconstituted enzyme (30 : 1) were generated in liposome buffer B (100 mM Tris, 100 mM maleic acid, 5 mM $MgCl_2$, 200 mM NaCl, pH 7.3) resulting in a concentration of 200 mM NaCl on the inside. The buffer on the outside was exchanged after centrifugation of the liposomes. The liposomes were resuspended in ATP synthesis buffer (100 mM Tris, 100 mM maleic acid, 5 mM $MgCl_2$, 10 mM NaCl, 200 mM KCl, 5 mM KH_2PO_4, pH 7.3) resulting in an outside concentration of 10 mM NaCl, thus creating a sodium ion potential (ΔpNa). Upon addition of 2 μM valinomycin and 5 mM ADP, a membrane potential ($\Delta\Psi$) was induced and the reaction was started. ATP synthesis was measured at 37 °C, and ATP was determined by luciferin–luciferase assay (blue, circles). In the red plot (triangles up), no ADP was added. Each value represents the mean and standard deviation of three independent experiments (n = 3).

GmbH, Dreieich, Germany). All preparations were routinely analyzed by SDS/PAGE, using the buffer system of Schägger and von Jagow [39]. Proteins were visualized by staining with Coomassie brilliant blue G250 (Sigma-Aldrich Chemie GmbH, Steinheim, Germany) [40].

Antibody generation and western blot

For expression of genes encoding for the single subunits A, B, C, D, and E, the amplified fragment was cloned into pTrc99a and each corresponding plasmid was transformed in *Escherichia coli* DK8. *E. coli* cultures were grown in 2xYT medium at 37 °C, and gene expression was induced at an OD_{600} of 1.0 by addition of 1 mM isopropyl-β-D-1-thiogalactopyranoside (IPTG). After 4 h of growth, cells were harvested, washed, and disrupted by a French press. After removal of cell debris, each single subunit was purified by Ni^{2+}-NTA chromatography. All subunits were separated and analyzed by SDS/PAGE, using the buffer system of Schägger and von Jagow [39] and visualized by staining with Coomassie brilliant blue G250 (Sigma-Aldrich Chemie GmbH) [40]. The subunits cut from a Coomassie-stained SDS gel were used to immunize rabbits. Western blotting with SDS/PAGE gels was performed as described previously [41].

Determination of ATPase activity

The ATPase activity of washed membranes isolated from cells grown on different substrates was measured in a buffer containing 100 mM Tris, 100 mM maleic acid, 10 mM $MgCl_2$, 20% methanol (v/v), pH 7.3. After incubation for 3 min at 37 °C, the reaction was started by the addition of 2.5 mM Na_2-ATP. The ATPase activity was determined by a discontinuous assay following the ATP-dependent formation of inorganic phosphate, according to the method of Heinonen and Lahti [42], as previously described [43]. To determine the effect of pH and temperature, the enzyme was preincubated for 3 min at the pH (5–9) or temperature (20–50 °C) indicated, respectively. The reaction temperature for the determination of the pH optimum was set to 37 °C. The buffer used for the pH optima determination was 50 mM MES, 50 mM Tris, 50 mM HEPES, 50 mM CHES, 10 mM $MgCl_2$, 20% methanol. For inhibitor studies with *N*′,*N*′-dicyclohexylcarbodiimide (DCCD), the reaction mixture was preincubated at room temperature for 30 min before the reaction was started by addition of Tris-ATP. For determination of ATPase activity in the absence of sodium ions, the activity was determined in 100 mM Tris/HCl, 5 mM $MgCl_2$, and 20% methanol as described above.

Labeling with NCD-4

Purified ATP synthase was labeled with NCD-4 (solved in ethanol) by incubation with 60 or 200 nmol of NCD-4 overnight at room temperature in the presence or absence of 200 nM NaCl. After incubation, the protein was separated by SDS/PAGE (12.5%) and fluorescence was detected after excitation with UV light.

Reconstitution of the A_1A_O ATP synthase in proteoliposomes

The reconstitution of the A_1A_O ATP synthase from *E. limosum* in unilamellar vesicles of phosphatidylcholine type II S from soybeans (Sigma-Aldrich Chemie GmbH) was carried out as for the ATP synthase from *A. woodii*, according to Ref. [27] with slight modifications. In order to solve phosphatidylcholine type II S from soybeans, either liposome buffer A (50 mM Tris/HCl, 10 $MgCl_2$, pH 7.5) or, for the determination of $\Delta\mu Na^+$-driven ATP synthesis, liposome buffer B (100 mM Tris, 100 mM maleic acid, 5 mM $MgCl_2$, 200 mM NaCl, pH 7.3) was used.

Measurement of $^{22}Na^+$ translocation

Na^+ translocation experiments in proteoliposomes were performed according to Ref. [27] in a buffer composed of 50 mM Tris/HCl, 10 mM $MgCl_2$, pH 7.3. The sodium ionophore ETH 2120 and the protonophore TCS were added from ethanolic stock solutions and controls received the

solvent only [final concentration: 0.3% (v/v)]. The proteoliposomes, the buffer, supplements, and $^{22}NaCl$ (carrier-free, final activity 0.5 $\mu Ci \cdot mL^{-1}$) were combined in a reaction tube to a final Na^+ concentration of 4.5 mM and incubated at 37 °C for 30 min to assure equilibration of $^{22}Na^+$, before the reaction was started by addition of 2.5 mM Tris-ATP (final concentration). Eighty microlitre samples were withdrawn and passed over a column (0.5 × 3.2 cm) of Dowex 50-WX8 (100–200-mesh) [43]. The proteoliposomes were collected by washing the column with 1 mL of 420 mM sucrose. The radioactivity in the eluate was determined by liquid scintillation counting.

Determination of ATP synthesis

To generate a $\Delta\mu Na^+$, the purified ATP synthase was first reconstituted with liposome buffer B (100 mM Tris, 100 mM maleic acid, 5 mM $MgCl_2$, 200 mM NaCl, pH 7.3) as described above. The loaded proteoliposomes were collected by extract (Beckman Optima L90-K, 70.2 Ti rotor, 150 000 ***g***, 30 min), washed once with ATP synthesis buffer (100 mM Tris, 100 mM maleic acid, 5 mM $MgCl_2$, 10 mM NaCl, 200 mM KCl, 5 mM KH_2PO_4, pH 7.3 (30 min, 150 000 ***g***, 30 min), and resolved in the same buffer. ATP synthesis of the reconstituted ATP synthase was started by addition of 2 μM valinomycin (Sigma-Aldrich) to induce a $\Delta\Psi$, 5 mM ADP (final concentration each) and measured by a standard luciferin/luciferase assay (Sigma-Aldrich) at 37 °C, monitoring the emitted light with a chemiluminometer (Berthold Technologies, Bad Wildbad, Germany) as described by Ref. [44].

Acknowledgements

Financial support by the Deutsche Forschungsgemeinschaft via SFB807 is gratefully acknowledged.

Conflict of interest

The authors declare no conflict of interest.

Author contributions

VM designed the experiments. DL performed the experiments. VM and DL analyzed the data. VM and DL wrote the paper.

References

1 Senior AE (1988) ATP synthesis by oxidative phosphorylation. *Physiol Rev* **68**, 177–231.
2 Müller V & Grüber G (2003) ATP synthases: structure, function and evolution of unique energy converters. *Cell Mol Life Sci* **60**, 474–494.
3 Cross RL & Müller V (2004) The evolution of A-, F-, and V-type ATP synthases and ATPases: reversals in function and changes in the H^+/ATP stoichiometry. *FEBS Lett* **576**, 1–4.
4 Stock D, Gibbons C, Arechaga I, Leslie AG & Walker JE (2000) The rotary mechanism of ATP synthase. *Curr Opin Struct Biol* **10**, 672–679.
5 Forgac M (2007) Vacuolar ATPases: rotary proton pumps in physiology and pathophysiology. *Nat Rev Mol Cell Biol* **8**, 917–929.
6 Grüber G, Manimekalai MS, Mayer F & Müller V (2014) ATP synthases from archaea: the beauty of a molecular motor. *Biochim Biophys Acta* **1837**, 940–952.
7 Müller V (2004) An exceptional variability in the motor of archaeal A_1A_O ATPases: from multimeric to monomeric rotors comprising 6–13 ion binding sites. *J Bioenerg Biomembr* **36**, 115–125.
8 Müller V, Lemker T, Lingl A, Weidner C, Coskun Ü & Grüber G (2005) Bioenergetics of archaea: ATP synthesis under harsh environmental conditions. *J Mol Microbiol Biotechnol* **10**, 167–180.
9 Mandel M, Moriyama Y, Hulmes JD, Pan Y-CE, Nelson H & Nelson N (1988) cDNA sequence encoding the 16-kDa proteolipid of chromaffin granules implies gene duplication in the evolution of H^+-ATPases. *Proc Natl Acad Sci USA* **85**, 5521–5524.
10 Nelson N (1992) Evolution of organellar proton-ATPases. *Biochim Biophys Acta* **1100**, 109–124.
11 Lim JK, Mayer F, Kang SG & Müller V (2014) Energy conservation by oxidation of formate to carbon dioxide and hydrogen via a sodium ion current in a hyperthermophilic archaeon. *Proc Natl Acad Sci USA* **111**, 11497–11502.
12 Pisa KY, Huber H, Thomm M & Müller V (2007) A sodium ion-dependent A_1A_O ATP synthase from the hyperthermophilic archaeon *Pyrococcus furiosus*. *FEBS J* **274**, 3928–3938.
13 Vonck J, Pisa KY, Morgner N, Brutschy B & Müller V (2009) Three-dimensional structure of A_1A_O ATP synthase from the hyperthermophilic archaeon *Pyrococcus furiosus* by electron microscopy. *J Biol Chem* **284**, 10110–10119.
14 Lingl A, Huber H, Stetter KO, Mayer F, Kellermann J & Müller V (2003) Isolation of a complete A_1A_O ATP synthase comprising nine subunits from the hyperthermophile *Methanococcus jannaschii*. *Extremophiles* **7**, 249–257.
15 Mayer F, Lim JK, Langer JD, Kang SG & Müller V (2015) Na^+ transport by the A_1A_O-ATP synthase purified from *Thermococcus onnurineus* and reconstituted into liposomes. *J Biol Chem* **290**, 6994–7002.
16 Kreuter LJ, Weinfurtner A, Ziegler A, Weigl J, Hoffmann J, Morgner N, Müller V & Huber H (2019) Purification of a crenarchaeal ATP synthase in

the light of the unique bioenergetics of *Ignicoccus* species. *J Bacteriol* **201**, 510–518.
17 Jeong J, Bertsch J, Hess V, Choi S, Choi IG, Chang IS & Müller V (2015) Energy conservation model based on genomic and experimental analyses of a carbon monoxide-utilizing, butyrate-forming acetogen, *Eubacterium limosum* KIST612. *Appl Environ Microbiol* **81**, 4782–4790.
18 Wilms R, Freiberg C, Wegerle E, Meier I, Mayer F & Müller V (1996) Subunit structure and organization of the genes of the A_1A_O ATPase from the archaeon *Methanosarcina mazei* Gö1. *J Biol Chem* **271**, 18843–18852.
19 Mayer F, Leone V, Langer JD, Faraldo-Gómez JD & Müller V (2012) A *c* subunit with four transmembrane helices and one ion (Na^+) binding site in an archaeal ATP synthase: implications for *c* ring function and structure. *J Biol Chem* **287**, 39327–39337.
20 Inatomi KI, Eya S, Maeda M & Futai M (1989) Amino acid sequence of the alpha and beta subunits of *Methanosarcina barkeri* ATPase deduced from cloned genes. *J Biol Chem* **264**, 10954–10959.
21 Anthon GE & Jagendorf AT (1983) Effect of methanol on spinach thylakoid ATPase. *Biochim Biolphys Acta* **723**, 358–363.
22 Hermolin J & Fillingame RH (1989) H^+-ATPase activity of *Escherichia coli* F_1F_O is blocked after reaction of dicyclohexylcarbodiimide with a single proteolipid (subunit *c*) of the F_O complex. *J Biol Chem* **264**, 3896–3903.
23 Altendorf K (1977) Purification of the DCCD-reactive protein of the energy-transducing adenosine triphosphatase complex from *Escherichia coli*. *FEBS Lett* **73**, 271–275.
24 McMillan DGG, Ferguson SA, Dey D, Schröder K, Aung HL, Carbone V, Attwood GT, Ronimus RS, Meier T, Janssen PH *et al*. (2011) A1Ao-ATP synthase of *Methanobrevibacter ruminantium* couples sodium ions for ATP synthesis under physiological conditions. *J Biol Chem* **286**, 39882–39892.
25 Laubinger W & Dimroth P (1988) Characterization of the ATP synthase of *Propionigenium modestum* as a primary sodium pump. *Biochemistry* **27**, 7531–7537.
26 Spruth M, Reidlinger J & Müller V (1995) Sodium ion dependence of inhibition of the Na^+-translocating F_1F_O-ATPase from *Acetobacterium woodii*. Probing the site (s) involved in ion transport. *Biochim Biolphys Acta* **1229**, 96–102.
27 Brandt K, Müller DB, Hoffmann J, Hübert C, Brutschy B, Deckers-Hebestreit G & Müller V (2013) Functional production of the Na^+ F_1F_O ATP synthase from *Acetobacterium woodii* in *Escherichia coli* requires the native AtpI. *J Bioenerg Biomembr* **45**, 15–23.
28 Deppenmeier U & Müller V (2008) Life close to the thermodynamic limit: how methanogenic archaea conserve energy. *Results Probl Cell Differ* **45**, 123–152.
29 Thauer RK, Kaster AK, Seedorf H, Buckel W & Hedderich R (2008) Methanogenic archaea: ecologically relevant differences in energy conservation. *Nat Rev Microbiol* **6**, 579–591.
30 Mayer F & Müller V (2013) Adaptations of anaerobic archaea to life under extreme energy limitation. *FEMS Microbiol Rev* **38**, 449–472.
31 Kim YJ, Lee HS, Kim ES, Bae SS, Lim JK, Matsumi R, Lebedinsky AV, Sokolova TG, Kozhevnikova DA, Cha SS *et al*. (2010) Formate-driven growth coupled with H_2 production. *Nature* **467**, 352–355.
32 Schlegel K & Müller V (2013) Evolution of Na^+ and H^+ bioenergetics in methanogenic archaea. *Biochem Soc Trans* **41**, 421–426.
33 Müller V & Hess V (2017) The minimum biological energy quantum. *Front Microbiol* **8**, 2019.
34 Cossio P, Allegretti M, Mayer F, Muller V, Vonck J & Hummer G (2018) Bayesian inference of rotor ring stoichiometry from electron microscopy images of archaeal ATP synthase. *Microscopy* **67**, 266–273.
35 Balch WE, Schoberth S, Tanner RS & Wolfe RS (1977) *Acetobacterium*, a new genus of hydrogen-oxidizing, carbon dioxide-reducing, anaerobic bacteria. *Int J Syst Bact* **27**, 355–361.
36 Spahn S, Brandt K & Müller V (2015) A low phosphorylation potential in the acetogen *Acetobacterium woodii* reflects its lifestyle at the thermodynamic edge of life. *Arch Microbiol* **197**, 745–751.
37 Matthies D, Zhou W, Klyszejko AL, Anselmi C, Yildiz O, Brandt K, Müller V, Faraldo-Gomez JD & Meier T (2014) High-resolution structure and mechanism of an F/V-hybrid rotor ring in a Na^+-coupled ATP synthase. *Nat Commun* **5**, 5286.
38 Chang IS, Kim BH, Kim DH, Lovitt RW & Sung HC (1999) Formulation of defined media for carbon monoxide fermentation by *Eubacterium limosum* KIST612 and the growth characteristics of the bacterium. *J Biosci Bioeng* **88**, 682–685.
39 Schägger H & von Jagow G (1987) Tricine-sodium dodecyl sulfate-polyacrylamide gel electrophoresis for the separation of proteins in the range from 1 to 100 kDa. *Anal Biochem* **166**, 369–379.
40 Weber K & Osborne M (1969) The reliability of the molecular weight determination by dodecyl sulfate polyacrylamide gel electrophoresis. *J Biol Chem* **244**, 4406–4412.
41 Towbin H, Staehelin T & Gordon J (1979) Electrophoretic transfer of proteins from polyacrylamide gels to nitrocellulose sheets: procedure and some applications. *Proc Natl Acad Sci USA* **76**, 4350–4354.
42 Heinonen JE & Lahti RJ (1981) A new and convenient colorimetric determination of inorganic orthophosphate

and its application to the assay of inorganic pyrophosphatase. *Anal Biochem* **113**, 313–317.

43 Heise R, Müller V & Gottschalk G (1992) Presence of a sodium-translocating ATPase in membrane vesicles of the homoacetogenic bacterium *Acetobacterium woodii*. *Eur J Biochem* **206**, 553–557.

44 Fritz M & Müller V (2007) An intermediate step in the evolution of ATPases – the F_1F_O-ATPase from *Acetobacterium woodii* contains F-type and V-type rotor subunits and is capable of ATP synthesis. *FEBS J* **274**, 3421–3428.